Geomechanics and Engineering, *Vol. 32, No. 1 (2023) 21-34*
https://doi.org/10.12989/gae.2023.32.1.021

Single piles under cyclic lateral loads - Full scale tests and numerical modelling

Hocine Haouari* and Ali Bouafia

Laboratory NEIGE, Department of civil engineering, Faculty of Technology, University of Blida, Route de Soumâa, P.O.Box 270, R.P Blida, 09000, Blida, Algeria

(*Received March 7, 2022, Revised December 15, 2022, Accepted December 17, 2022*)

Abstract. In order to analyze the effect of the cyclic lateral loading on the response of a pile-soil system, a full-scale single steel pile was subjected to one-way cyclic loading. The test pile was driven into a bi-layered soil consisting of a normally consolidated saturated clay overlying a silty sandy layer, the site being submerged by water up to one meter above the mudline in order to reproduce the conditions of an offshore pile foundation. The aim of this paper is to present the main results of interpretation of the cyclic lateral tests in terms of pile deflections, bending moment, and cyclic P-Y curves. From these latter an absolute secant reaction modulus $E_{AS,N}$ was derived and a simple calculation model of the test single pile is proposed based on this modulus. Two applications of the proposed model are carried out, one with a 2D finite element modelling, and the second with a load transfer curves-based method.

Keywords: absolute secant modulus of lateral reaction; bi-layered soil; cyclic lateral loading; full-scale test; P-Y curves; single pile

1. Introduction

A single pile may be subjected to lateral monotonic loading (Fenu *et al*. 2019, Adeel *et al.* 2022), as well as lateral cyclic loading, for example, monopile foundations of offshore structures which are exposed to a very large number of loading-unloading cycles mainly induced by the wind and waves forces (Chong *et al.* 2019, Barari *et al*. 2021, Staubach *et al*. 2021). Lateral cyclic loading generally has an unfavourable effect on the pile lateral response compared to the monotonic loading. This effect is mainly reflected in an increase in the pile deflections and rotation. This has commonly been explained in terms of two main phenomena: the accumulation of deformations without change in soil properties called “structural shakedown”, and the degradation of the soil material resulting in a decrease in its strength and stiffness (Poulos 1988, Swane 1983). The progressive formation of a gap near the ground surface at the pile-soil interface is another phenomenon that may occur to increase the cyclic effect especially in cases of cohesive soils (Allotey and El Naggar 2008, Tuladhar *et al*. 2008).

However, the rate of accumulation of permanent deformations and cyclic deflections tends to decrease with cycling, this means that the reloading stiffness has to be higher than the prior loading stiffness, and also increases for subsequent cycles (Rosquoët *et al*. 2007, Hinz 2009).

This divergence between material degradation and cyclic stiffening is most likely due to incoherence in terminology used in the literature, where the term "stiffness" is overused without specifying whether the absolute secant, the relative or the tangent stiffness is intended.

In fact, the absolute secant stiffness, expressed as the ratio of the applied load to the absolute displacement, will always have a degrading character. On the other hand, the relative stiffness will generally increase with cycling, particularly with cohesionless soils. (LeBlanc *et al*. 2010, Klinkvort and Hededal 2013, Abadie and Byrne 2014, Nicolai and Ibsen 2015, Chiou *et al*. 2018).

The cyclic behaviour of single piles depends on many factors such as the cyclic load level or the loading amplitude, the number of cycles, the type of cyclic loading (i.e. one-way or two-way, regular or irregular,…etc), the frequency of loading, and other factors such as the soil type and the pile material properties (Cuéllar 2011).

An important experimental research program on the monotonic and cyclic behaviour of piles under cyclic loading was undertaken by the IFSTTAR (formerly: LCPC Laboratories) and the IFP (Institut Français du Pétrole) by means of full-scale tests. This paper aims to present a detailed interpretation of the results of field lateral load tests on a single pile driven in a saturated two-layer soil situated in Plancoet (France). After a brief review of existing calculation methods of single piles subjected to cyclic lateral loads, and a brief description of the test pile, its instrumentation, and the geotechnical aspects of the experimental site, the main results are presented focusing on the pile head deflection, the maximum bending moment, and the cyclic P-Y curves. In the last part of the paper, a calculation model for a single pile under cyclic lateral loading is proposed and two applications of this model are carried out, one based on a 2D finite element modeling

*Corresponding author, Mr.
E-mail: haouari.ce.geo@gmail.com

ISSN: 2005-307X (Print), 2092-6219 (Online)

using ABAQUS software, and the other based on the load transfer curves method using IGtHPile software.

2. Brief review of earlier works

Two main approaches can be observed to consider the effects of cyclic loading on the behavior of the single pile-soil system: the empirical methods for estimating the pile head deflection and/or the rotation, and the maximum bending moment in the pile, and the modified P-Y curves - based method by reducing the soil lateral reaction. We may also indicate the extended strain wedge (SW) model and the application of high-cycle accumulation (HCA) model.

2.1 Empirical methods

For sand as well as for clay, earlier studies showed that cyclic lateral loading generally leads to an increase in pile head deflection with the number of cycles, this displacement may be approximately estimated either by logarithmic or power functions, such as:

Logarithmic function

$$Y_N = Y_1 \cdot (1 + t \cdot \ln N) \tag{1}$$

Power functions

$$Y_N = Y_1 \cdot N^m \tag{2}$$

Where:
Y_N: pile head deflection after N cycles,
Y_1: pile head deflection after one cycle,
t and m: degradation parameters.

(Hettler 1981) conducted loading tests on small scale models of flexible piles embedded in dry sand. The results lead to a degradation parameter t=0.2. (Bouafia 1994) carried out cyclic loading tests on centrifuged small-scale models of two piles (one flexible and one rigid) embedded in a dry poorly graded dense sand and the results analysis led to t values ranging between 0.18 and 0.25. Based on results of various cyclic loading tests on piles installed in sandy soils, (Lin and Liao 1999) found that the parameter t depends on soil density, pile installation method, cyclic loading type, pile embedded length, and pile/soil relative stiffness ratio, as follows

$$t = 0.032 \frac{D}{K_R} F_L \, F_I \, F_D \tag{3}$$

Where:
D: the pile embedded length,
K_R: the pile/soil relative stiffness ration,
$K_R = (E_p I_p / n_h)^{0.2}$, E_p: pile modulus of elasticity, I_p: pile moment of inertia, and n_h: subgrade reaction coefficient.
F_L: influence factor of the cyclic load ratio, R_H
$R_H = H_{min}/H_{max}$, H_{min} and H_{max}: minimum and maximum cyclic loading levels,
F_I: influence factor of pile installation method,
F_D: influence factor of soil density.

For medium to dense sands, (Rosquoët *et al.* 2007) expressed the parameter t by power function in terms of the cyclic component, H'_{cyc} ($H'_{cyc} = H_{max-min}$), and the maximum cyclic loading level, H_{max}, such as:

$$t = 0.08 \left(\frac{H'_{cyc}}{H_{max}} \right)^{0.35} \tag{4}$$

Based on results of one way cyclic loading tests, $H_{min} = 0$, on 1-g small scale models of flexible piles embedded in dry medium dense sand, (Peralta 2010) reported that the degradation parameter $t=0.21$ and is independent of the maximum cyclic loading level , H_{max}.

(Long and Vanneste 1994) analysed results of 34 pile cyclic loading tests, undertaken on different sandy soils, with various pile length, and installation techniques, and based on closed-form solution for beam on elastic foundation where the subgrade reaction modulus, E_{it} increase linearly with depth z with a slope, n_h named the sabgrade reaction coefficient ($E_{it} = n_h z$), they adopted the power approach to estimate pile head displacement under cyclic loading, for long flexible piles, they found that degradation parameter $m = 0.6\ \alpha$ for pure lateral force, and $m = 0.4\ \alpha$ for pure moment action on pile head, For one-way cyclic loading, m varies between m = 0.04 and $m = 0.16$, with:

$$\alpha = 0.17 F_L \, F_I \, F_D \tag{5}$$

(Peralta 2010) found that, contrarily to flexible piles, for rigid piles in dry sand, a power law matches better the test results, for one-way cyclic loading, $H_{min} = 0$, and a value of 0.12 is suggested for the degradation parameter m.

(Klinkvort and Hededal 2013) conducted cyclic loading on 1-g small scale models of rigid piles embedded in dry or saturated sand, they adopted the power law to estimate pile head displacement under one-way and two-way cyclic loading, the degradation parameter m is expressed as:

$$m = T_c \, T_b \tag{6}$$

T_c and T_b are influence factors that respectively depend on the cyclic load ratio, R_H, and the load magnitude ratio, H_{max} / H_u, where H_u is the monotonic lateral bearing capacity. The exponent, m, is proportional to load magnitude ratio, and the most unfavorable situation encountered with pure one-way loading, $H_{min} = 0$.

(Briaud 2013) proposed to calculate the exponent, m, in case of one-way cyclic loading from results of the cyclic pressuremeter test since the soil stress-strain behavior derived from expansion of the pressuremeter probe during cyclic pressuremeter test is quite similar to that derived from cyclic lateral loading of a single pile, such as

$$m = \frac{ln\left(\frac{E_N}{E_1} \right)}{ln(N)} \tag{7}$$

Where E_1 and E_N are the first load PMT moduli of the first cycle and the N^{th} cycle respectively. the exponent, m found to vary in the range of 0.01 to 0.35 in clays and that of 0.005 to 0.26 for sands.

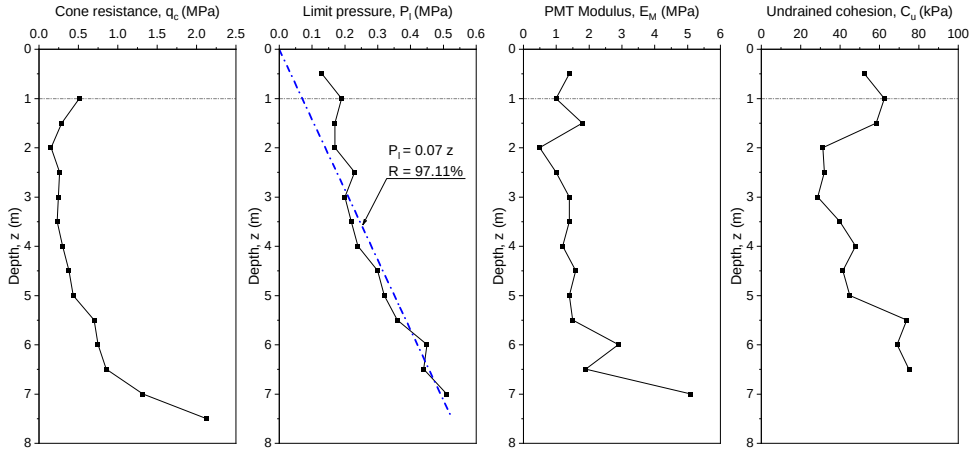

Fig. 1 Typical in-situ properties of the experimental site

2.2 Modified P-Y curves-based approach

This approach is based on modifying the monotonic P-Y curves to consider the effect of loading cycles, by reducing the soil lateral reaction. The P-Y curves method to analyse laterally loaded piles is often used in practice where the letter *P* denotes the soil lateral reaction while the letter *Y* designates the pile deflection. The proposed cyclic curves are in fact modified monotonic curves, (Gazioglu and O'Neill 1984,Matlock 1970,Reese *et al.* 1974, 1975, Reese and Welch 1975, Sullivan *et al.* 1980), the American Petroleum Institute (API 2007) method is the most widely used in practice where the P-Y curves were derived from full-scale field tests of maximum number of cycles, N = 100. For example, for sands the *P-Y* curves are given by the following expression

$$P = A P_u \tanh\left[\frac{n_h z}{A P_u} Y\right] \tag{8}$$

Where:

P_u: ultimate soil lateral reaction

A: empirical factor, where:

$A = (3{,}0 - 0{,}8 \cdot z/B) \geq 0{,}9$ for a static load,

$A = 0{,}9$ for a cyclic load.

It can be observed that A factor is constant and independent of the number of cycles and the cyclic loading characteristics. The ratio, A', indicates the reduction rate of the soil lateral reaction due to cyclic loading

$$A' = \frac{0.9}{\left(3 - 0.8\frac{z}{B}\right)} \tag{9}$$

The cyclic reduction rate in soil reaction is depth related function, with a maximum value of 30% at the soil surface, this reduction rate decreases gradually with the depth, z, to disappear at the relative depth z/B = 2.625 (Peralta 2010).

2.3 Extended SW model and HCA model

Besides the aforementioned approaches, there are other advanced approaches, which include mainly the extended strain wedge (SW) model and the high-cycle accumulation (HCA) model. The SW model was originally proposed by Norris (1986) and further developed by Ashour *et al.* (2000) This approach was then extended for cyclic loads by describing the soil triaxial stress-strain behaviour in the strain wedge with the hyperbolic model of Duncan–Chang 1970 (Taşan 2011, Yang *et al*. 2021).

Niemunis *et al.* (2005) originally developed the high-cycle accumulation (HCA) model with focus on sand under drained high cycle loading (millions of load cycles) assuming a constant strain amplitude. This model was subsequently enhanced to take into account the influence of rapid changes in soil stiffness on the strain amplitude as encountered, for example, in case of large changes ineffective stress during the high-cyclic loading. The enhanced HCA model was then applied to monopile foundations for offshore wind turbines (OWTs) under high-cyclic lateral loading and partially drained conditions (Staubach *et al.* 2021).

The HCA model developed by Niemunis *et al*. (2005) was also adapted to predict the accumulation of permanent deformations or excess pore water pressure in clay under a large number of load cycles (Staubach *et al.* 2022). As for the sand, it was applied to offshore wind turbine foundations under long-term lateral cyclic loading by the back-analysis of a centrifuge test on a monopile in soft clay.

3. Description of the field test arrangement

3.1 Geotechnical description of the experimental site

The experimental site is located in Plancoët (Côtes-du-Nord, France), 450 km west of Paris. The ground consists of a bi-layered deposit composed of a low plasticity clayey layer (CL), 4 m thick, overlying a layer of silty sand (SM), 4 m thick. Beyond this depth, the soil consists of a highly plastic clayey layer (CH). Due to its proximity to the river Arguenon, the site is submerged by the ground water, (Baguelin and Jezequel 1972).

A cone Penetration Test (CPT) was carried out before installation of the test pile by using a Gouda device, with a

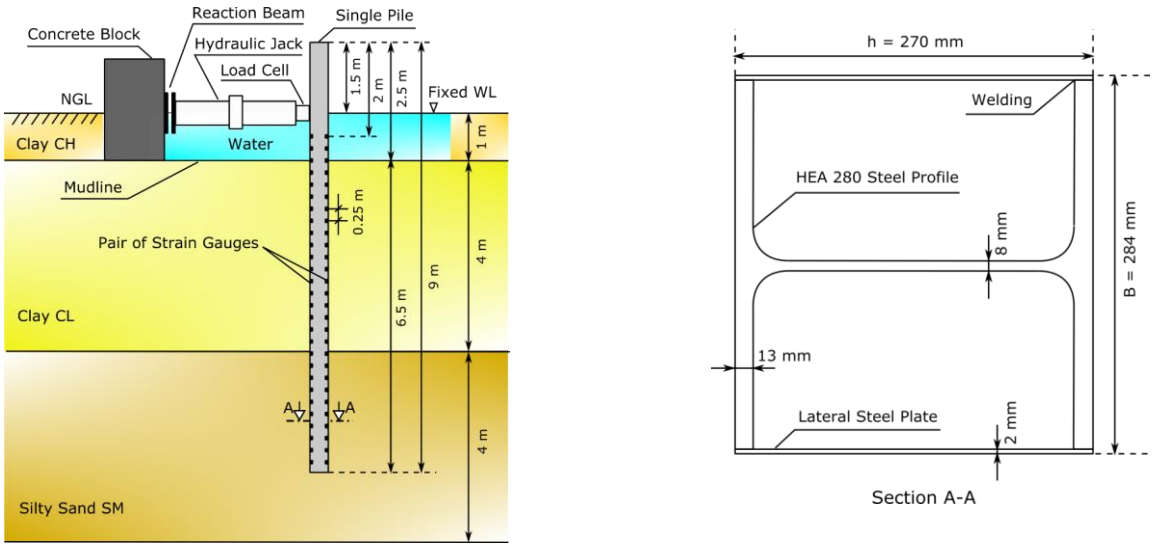

(a) Schematic of testing arrangement (b) Cross-section of the pile

Fig. 2 Test pile and loading device configuration

10 cm^2 standard electrical cone penetrating at a velocity of 20 mm/s. A prebored Pressuremeter Test (PMT) using an E standard probe in order to measure the limit pressure P_l and the PMT soil modulus E_M, as well as a Vane shear test (VST), were carried out before the installation of the test pile. The profiles of these tests are compiled in Fig. 1, it is clear that the limit pressure increases linearly with depth z, the gradient of increase equals to 0.07 MN/m^3.

The average values of the effective shear strength parameters (φ', c') of the clayey samples, obtained from a consolidated undrained triaxial shear tests (CU), are φ'=39.1° and c'=2 kPa.

As illustrated in Fig. 1, The (VST) undrained shear strength profile exhibits a linear trend similar to the profiles of the other mechanical properties, which is typical to a normally consolidated clay. Furthermore, this layer is classified as very soft to soft clay based on the margins of the limit pressure, the PMT modulus and the cone resistance (AFNOR 2012, CCTG 1993, Ménard 1967). However, the margin values of 20-75 kPa obtained for C_u, classify the soil as a soil of low to medium resistance (AFNOR 2005). On the other hand, the ratio E_M/P_l which is equivalent to a soil rigidity index according to the pressuremeter theory of Ménard, inventor of the PMT test, classify the soil to be a under-consolidated to normally consolidated clay, (Cassan 1978, CCTG 1993).

The friction angle value of the sandy layer is equal to 33° indicating a medium dense sand. As shown in Fig. 1, according to the PMT data and the Cone Penetration Test (CPT) data, the sandy layer is classified as loose to medium dense, (AFNOR 2012; CCTG 1993). However, the margins of the ratio E_M/P_l classify the soil as a loose to medium dense sand, (CCTG 1993).

After pile driving and prior to pile loading tests, the soil layer, from the natural ground level (NGL) and down to a one-meter depth, which consists of a highly plastic clayey layer (CH), was removed in order to eliminate this layer over-consolidated by desiccation which would complicate the interpretation of the results. Indeed, according to previous works, (Baguelin and Jezequel 1972, Reese and Impe 2010, Smith 1983) shallow depths of a clayey layer are usually over-consolidated by seasonal desiccation and exhibit a relatively much higher stiffness values than the deeper ones, which is not representative of the soil underneath.

The excavation was subsequently submerged, and the water level (WL) was maintained at the natural ground level (NGL) during all the experimentation in order to simulate the real conditions of pile foundations in an off-shore structure (Baguelin *et al*. 1985, Hadjadji *et al*. 2002).

3.2 Pile description and instrumentation

As illustrated in Fig. 2, the test pile is an HEA-280 steel profile on which two steel plates were welded on its lateral sides which results in a rectangular 0.27x0.28 m pile, the lateral load is applied parallel to these plates. The pile has a length (L) of 9 m, a width (B) of 0.284 m, an embedded length (D) of 6.5 m and a slenderness ratio (D/B) of 22.8. The overall flexural stiffness of the pile section is 30 MN.m^2 and the yielding bending moment of the pile is 285 kN.m (Baguelin *et al*. 1989).

The test pile was instrumented by 28 pairs of strain gauges fixed along two opposite vertical axes inside the pile. The Gauges distribution, started 0.5 m above the mudline (bottom of the excavation) with an increment of 0.25 m. The two first gauges were therefore out of the embedded pile length. Moreover, pile deflections were measured by 4 LVDTs (Linear Variable Displacement Transducer) fixed on the pile at 1.10 and 1.6 m above the mudline, as depicted in Fig. 2. The average pile displacements measured at two levels above the lateral load were useful for the integration procedure of bending moments to obtain the pile deflections, which requires two boundary conditions.

The lateral loads were applied at 1 m above mudline,

Table 1 Programme of lateral loading at the site Plancoët

Test type	Time elapsed after previous test (in days)	Test duration (in hours)	Number of cycles	Applied loads (kN)
Short static	274 after driving	8 (2 hours per increment)	---	5, 10, 15 then 20
Maintained static	---	1106 (46 days)	---	20
Cyclic	108	4	1000	7.55 - 14.28

measured by a load cell incorporated between the hydraulic jack and the pile head, and provided by a double- effect hydraulic jack powered by either a low powered hydraulic plant adapted to maintain constant the applied monotonic loads, or by a highly powered hydraulic plant adapted to high frequency cyclic loads (Meimon *et al.* 1986). The two gauges above the mudline served also to check the applied lateral load. As shown in Fig. 2, the jack was connected to a concrete mass via a reaction beam (Degny *et al*. 1994).

The pile was closed ended and submitted to a procedure of driving by a DELMAG- D5 hammer which likely induced high pressures to the surrounding soil, but as indicated in table 1, the time elapsed between the pile driving and the first loading tests was 274 days which is judged sufficient for a total dissipation of the excess pore pressures within the soil (Baguelin and Jezequel 1972).

3.3 Experimental programme of loading

The lateral loading tests consist of 3 sequences of loadings. As mentioned in Table 1, the first one involves a series of 4 monotonic loading stages, during 2 hours each, using a load increment of 5 kN. The loads are applied at a distance of 1 m above the mudline.

The second sequence consists of maintaining the 20 kN lateral loading during 46 days in order to study the evolution of the lateral load-deflection pile response with the time.

According to Table 1 and Fig. 3, the last sequence involves a series of one-way cyclic lateral loading carried out 108 days after unloading the pile. It consists of 1000 cycles, 14 seconds each, corresponding to a controlled loading frequency of 0.071 Hz. In this paper, the focus is restricted to the cyclic loading test.

It is to be noticed that continuous measurement of bending moments via the strain gauges during all the time of testing was unfortunately not possible since the strain gauges were disconnected for many times during the complete unloading phases. Thus, for a given test, the values of the bending moments are measured from the beginning of this test: they are therefore relative values and it is impossible to know their absolute values (it is impossible to take into account the residual bending moments existing in the pile before the beginning of the test). Consequently, the lateral displacements Y of the pile and the soil reactions P for each depth level are also relative values: the P-Y reaction curves will therefore be relative to the test involved and not to the whole stress history of the soil since the beginning of the test series.

On the other hand, it is possible to know the absolute values of the pile lateral displacements at the mudline

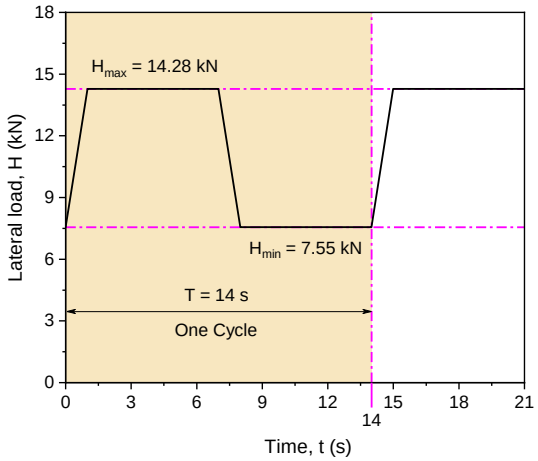

Fig. 3 Sequence of cyclic loading

because the displacement transducers at the pile head were continuously functional during the whole test series. However, it was preferred to present the relative values of these latter to avoid any ambiguity or incoherence with the relative values of lateral displacement, bending moment, and soil reaction for each depth level.

4. Presentation and discussion of results

4.1 Pile bending moment

The experimental bending moment M(z) is calculated from the axial strain measurements ε(z), these latter are obtained at each level of strain gauge pair, such as

$$M(z) = 2 E_p I_p \frac{\varepsilon(z)}{B} \tag{10}$$

The experimental bending moment profiles thus found are smoothed by the Savitzky-Golay smoothing method which performs a local polynomial regression around each point and creates a new smoothed value for each data point, therefore, all singular points were eliminated; this method is used with a 3rd order regression polynomial, and 15 points for each local regression.

Fig. 4 shows the experimental bending moment profiles for the maximum and minimum cyclic loading levels, from cycle N = 1 through cycle N = 1000, where for clarity, only some cycles were illustrated.

4.1.1 Maximum bending moment

The Fig. 4 shows that bending moment profiles exhibit regular amplification up to 500 cycles, after which the

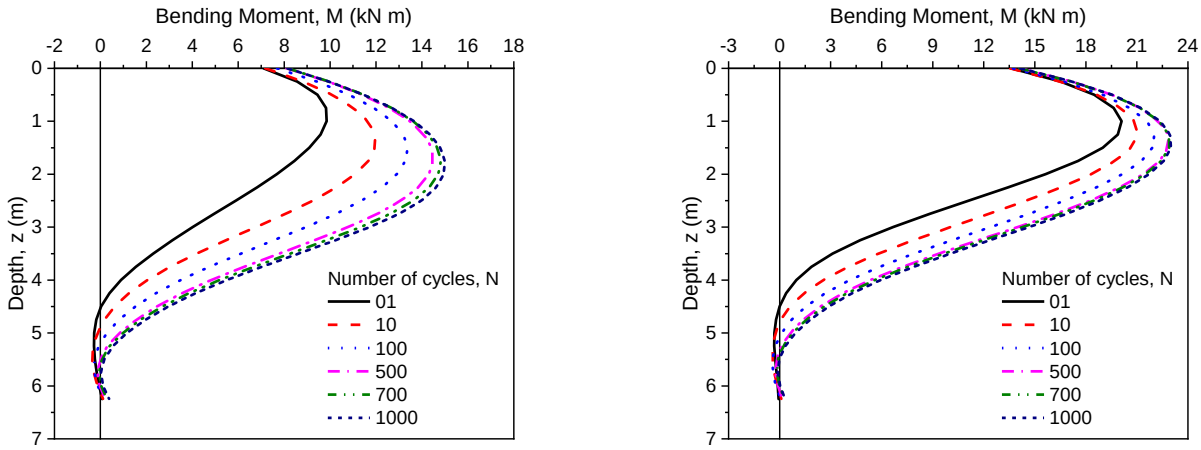

(a) Pile bending moment for H_{min} (b) Pile bending moment for H_{max}

Fig. 4 Experimental bending moment profiles

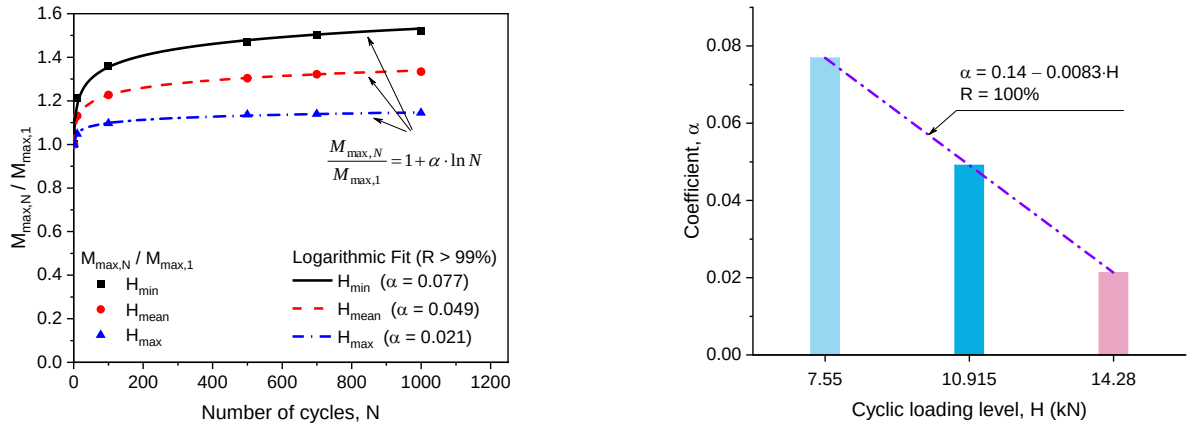

(a) Normalised M_{max} versus the number of cycles (b) Variation of the coefficient α versus load level

Fig. 5 Cyclic loading effect on the maximum bending moment M_{max}

profiles are very close, which is a sign of certain stabilisation. The evolution of the maximum bending moment M_{max} with regard to the number of cycles N is analysed in terms of the normalised maximum bending moment $M_{max,N}/M_{max,1}$, where $M_{max,N}$ and $M_{max,1}$ are respectively the maximum bending moment after N cycles and for the first cycle. Fig. 5(a) illustrates that the $M_{max,N}/M_{max,1}$ increases in a logarithmic form with the number of cycles N, with a fitting coefficient R > 99%, such as

$$\frac{M_{max,N}}{M_{max,1}} = 1 + \alpha \cdot \ln N \tag{11}$$

The coefficient α varies within the margin 0.021 – 0.077 as function of cyclic loading level and takes 0.049 for the mean load level, H_{mean}, this coefficient decreases linearly with the cyclic loading level, as shown in Fig. 5(b).

4.1.2 Depth of the Maximum bending Moment

Regarding the depth of the maximum bending moment, z_{Mmax}, we can see that z_{Mmax} is proportional to the number of cycles N, this is more significant in the case of the minimum load H_{min}, which can be explained by the rearrangement of the soil grains behind the pile due to the combined effect of soil weight and loading cycles, leading to an increase in soil reaction and consequently in the pile bending moment, the latter is deeper as the number of cycles N increases, which seems to be logic under the combined effect mentioned up above.

Fig. 6(a) depicts the dependence of normalised depth of maximum bending moment, z_{Mmax} / D on the number of cycles, N. We can observe that for both load levels (H_{min} and H_{max}), z_{Mmax} = 0.153D for the first cycle. After 1000 cycles, the value of z_{Mmax} increases to 0.270D for H_{min}, and 0.216D for the maximum load, H_{max}, with an average increase of 0.243D.

Given the shape of the increase, it was fitted by a logarithmic function with a fitting coefficient R ≥ 96%, such as

$$\frac{z_{M_{max}}}{D} = 0.153 + \beta \cdot \ln N \tag{12}$$

As shown in Fig. 6(b), the coefficient β is inversely proportional to the loading level, where it decreases linearly from the lower to the upper cyclic loading bound.

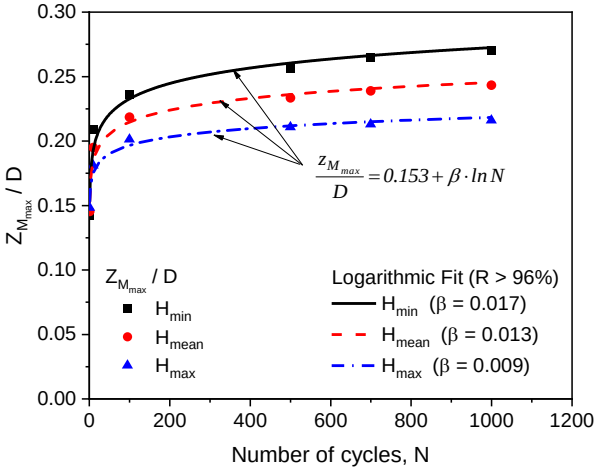

(a) Normalised Z_{Mmax} versus the number of cycles

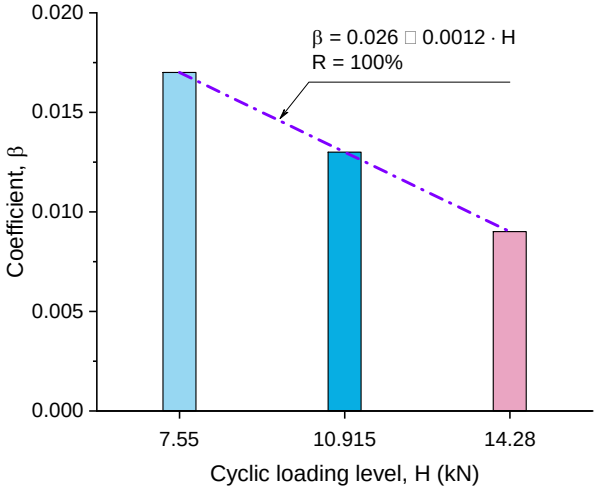

(b) Variation of the coefficient β versus load level

Fig. 6 Cyclic loading effect on the depth of the maximum bending moment Z_{Mmax}

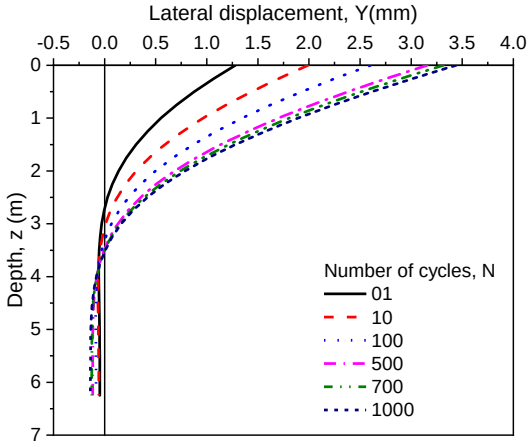

(a) Deflection for H_{min}

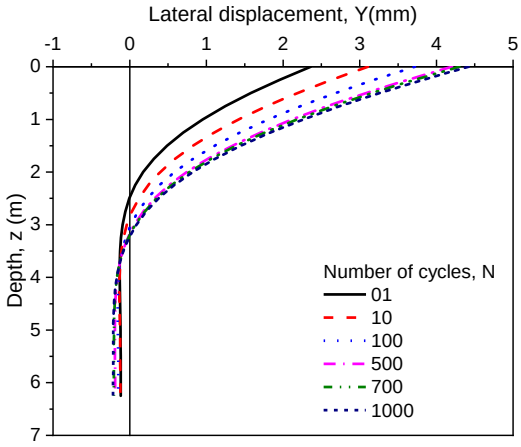

(b) Deflection for H_{max}

Fig. 7 Experimental displacement profiles

4.2 Pile deflection

The displacement measurements by LVDTs fixed on the pile head allowed the calculation of the pile rotation y'_0 and the pile deflection Y_0 at the mudline, these latter are required boundary conditions to calculate the pile shaft deflection $Y(z)$ by double integration of the bending moment (see Fig. 7), such as

$$Y(z) = \frac{1}{E_p I_p} \int_0^z \int_0^z M(z) dz dz + Y_0' z + Y_0 \qquad (13)$$

4.2.1 Cyclic force – Displacement curve at the mudline

Fig. 8(a) illustrates the Force-Displacement curve at mudline, where it can be seen that the mudline deflections ($Y_{0,max}$, $Y_{0,min}$) increase with the number of cycles N but tend to stabilise after 500 cycles, therefore the cyclic loops also stabilise, which is a sign of cyclic accommodation. A typical Force-Displacement curve with the same behaviour is shown in Fig. 8(b), the main characteristics of this curve are: the mudline lateral displacements ($Y_{0,max}$, $Y_{0,min}$), the pile absolute stiffness $K_{AH,N}$ and the pile relative stiffness $K_{RH,N}$.

The pile absolute stiffness is the ratio of the lateral force H to the mudline displacement Y_0 for N cycles (see Eq. (14)), while the pile relative stiffness is the ratio of the force levels difference ΔH to the mudline displacements difference ΔY_0 for N cycles (see Eq. (15)).

$$K_{AH,N} = \frac{H}{Y_{0,N}} \qquad (14)$$

$$K_{RH,N} = \frac{\Delta H}{\Delta Y_{0,N}} = \frac{H_{max} - H_{min}}{Y_{0,N}^{max} - Y_{0,N}^{min}} \qquad (15)$$

4.2.1.1 Pile displacements at the mudline

As shown in Fig. 9(a), the cumulative increase of mudline normalised displacements may be described by a logarithmic function, where $Y_{0,1}$ and $Y_{0,N}$ are respectively the mudline displacements at cycles 1 and N, such as

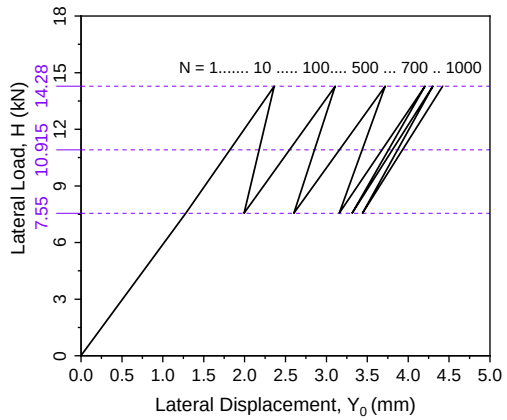

(a) Experimental cyclic *Force - Displacement* curve

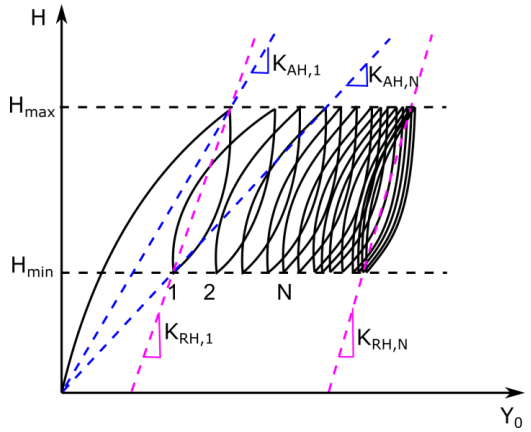

(b) Typical cyclic *Force - Displacement* curve

Fig. 8 Cyclic *Force - Displacement* curve at the mudline

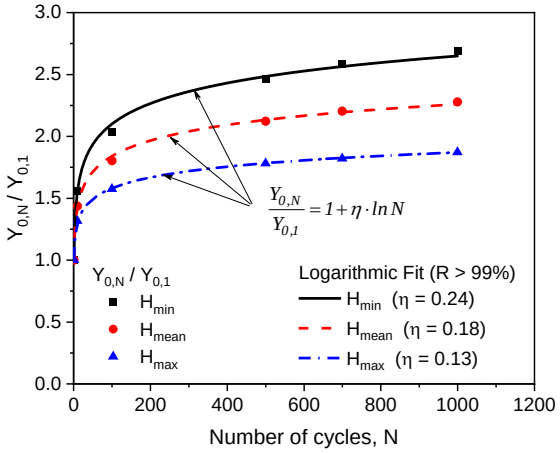

(a) Normalised pile displacement Y_0 versus the number of cycles

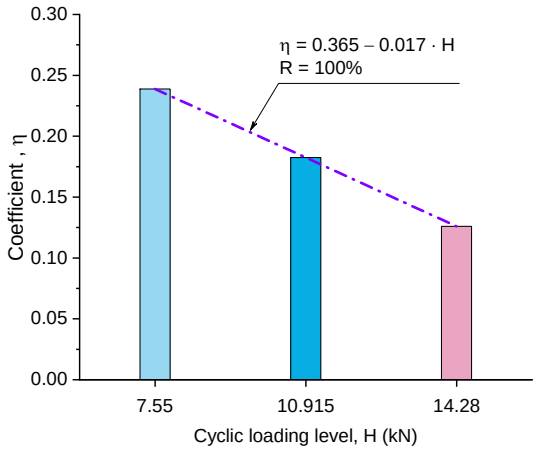

(b) Variation of the coefficient η versus load level

Fig. 9 Cyclic effect on the pile displacement at the mudline Y_0

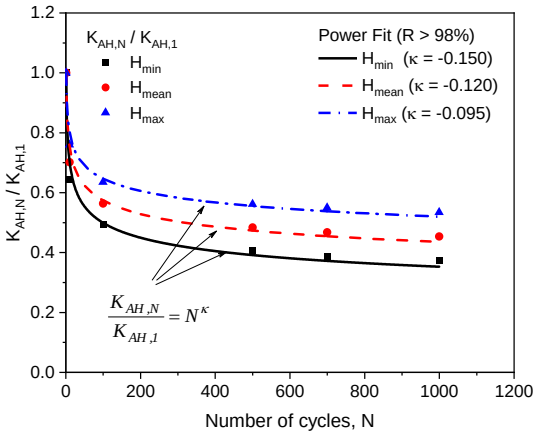

(a) Pile normalised absolute stiffness versus the number of cycles

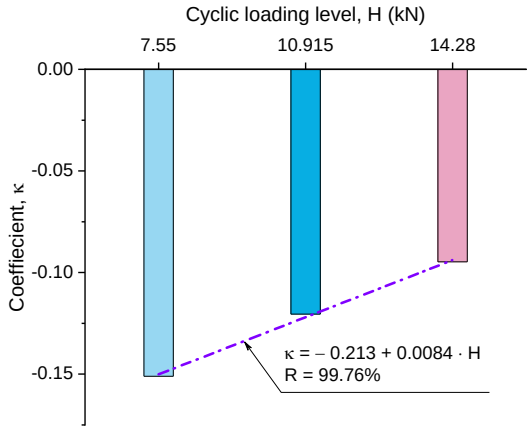

(b) Variation of the exponent κ versus load level

Fig. 10 Cyclic effect on the pile absolute stiffness

$$\frac{Y_{0,N}}{Y_{0,1}} = 1 + \eta \cdot \ln N \qquad (16)$$

Fig. 9(b) illustrates that the coefficient η, usually called the degradation factor, linearly decreases with the cyclic loading level and varies between 0.13 for H_{max} and 0.24 for H_{min}, with a value of 0.18 for H_{mean}. These margins are

comparable to those found elsewhere in sand, namely 0.20 (Hettler 1981), 0.18-0.25 (Bouafia 1994), 0.17-0.25 (Li *et al.* 2010) and 0.25 (Peralta 2010).

4.2.1.2 Pile absolute stiffness

The pile normalised absolute stiffness at the mudline $K_{AH,N}/K_{AH,1}$ degrades in power form with the number of cycles N, as shown in Fig. 10(a), this degradation is governed by the following equation

$$\frac{K_{AH,N}}{K_{AH,1}} = N^{\kappa} \tag{17}$$

The coefficient κ increases with the amplitude of the lateral loading, as illustrated by Fig. 10(b). The negative values taken by this coefficient indicates a cyclic degradation of the pile absolute stiffness.

4.2.1.3 Pile relative stiffness

The Fig. 11 illustrates that the pile normalised relative stiffness $K_{RH,N}/K_{RH,1}$ is almost constant with the number of cycles N, however it shows a slight increase which has a linear form, such as

$$\frac{K_{RH,N}}{K_{RH,1}} = 1 + 1.046 \times 10^{-4} \cdot N \tag{18}$$

4.3 Cyclic P-Y curves

The soil lateral reaction $P(z)$ is calculated by double differentiation of the bending moment $M(z)$ (see Eq. (19)), the Fig. 12 shows profiles of the soil lateral reaction along the pile shaft.

Knowing the pile deflection $Y(z)$ and soil lateral reaction $P(z)$ profiles along the pile shaft, the cyclic P-Y curves were constructed, as illustrated in Fig. 13, they are marked by an oscillating shape tending to stabilize. The whole points may be bounded by two envelopes. The first one corresponds to the points of H_{max} and tends to pass by a peak corresponding to about 15 kN/m then to stabilize towards an asymptote, whereas the second one corresponding to H_{min} is characterized by an asymptote of about 5 kN/m.

$$P(z) = -\frac{d^2 M}{dz^2} \tag{19}$$

The absolute secant reaction modulus $E_{AS,N}$ is defined at a given depth as the ratio of the soil reaction P_N at cycle N to the corresponding displacement Y_N, as follows

$$E_{AS,N} = \frac{P_N}{Y_N} \tag{20}$$

As illustrated by Fig. 14, the profiles of $E_{AS,N}$ for H_{max} or H_{min} exhibit linear variation with depth. Moreover, as shown in Fig. 15(a), for a given loading level, normalised absolute secant reaction modulus $E_{AS,N}$ / $E_{AS,1}$ decreases with number of cycles N, indicating an important cyclic degradation of the soil absolute lateral rigidity according to a power form as follows

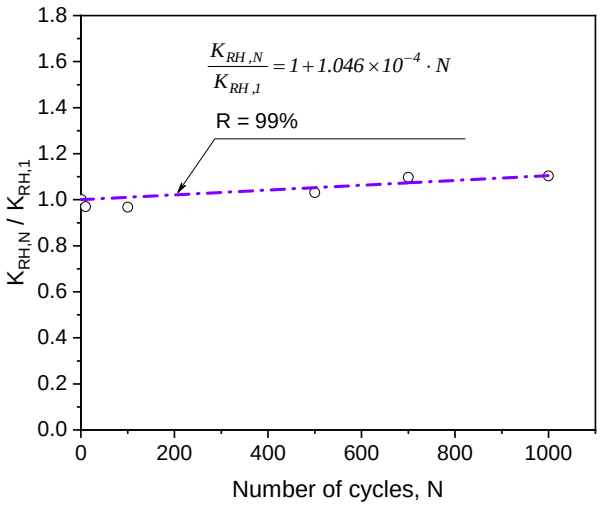

Fig. 11 Cyclic effect on the pile normalised relative stiffness

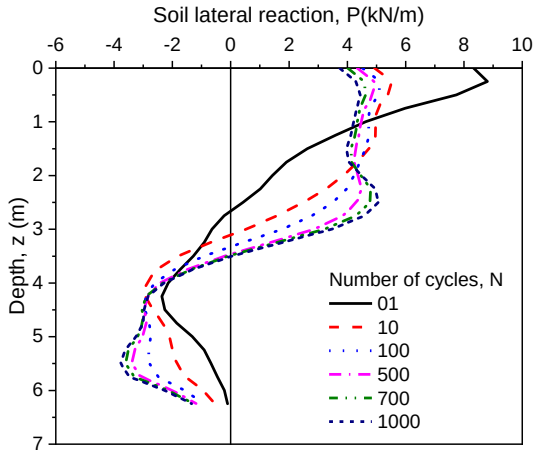

(a) Soil lateral reaction for H_{min}

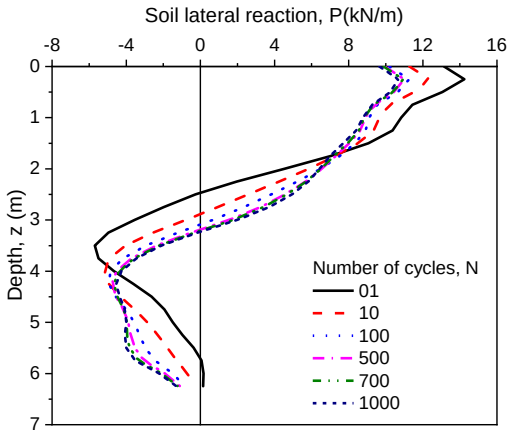

(b) Soil lateral reaction for H_{max}

Fig. 12 Soil lateral reaction profiles

$$\frac{E_{AS,N}}{E_{AS,1}} = N^{\xi} \tag{21}$$

The exponent ξ, as shown in Fig. 15(b), varies as linear function of the cyclic loading level, within a very narrow

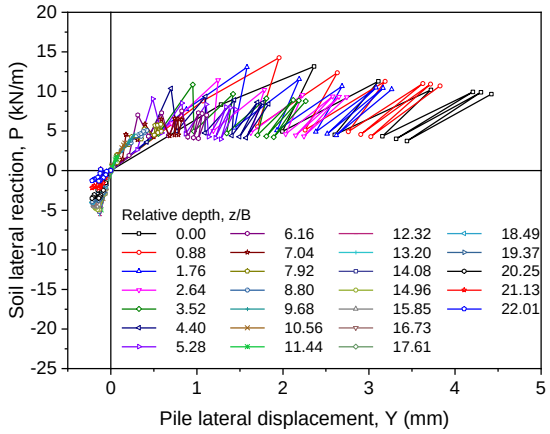

Fig. 13 Experimental cyclic P-Y curves

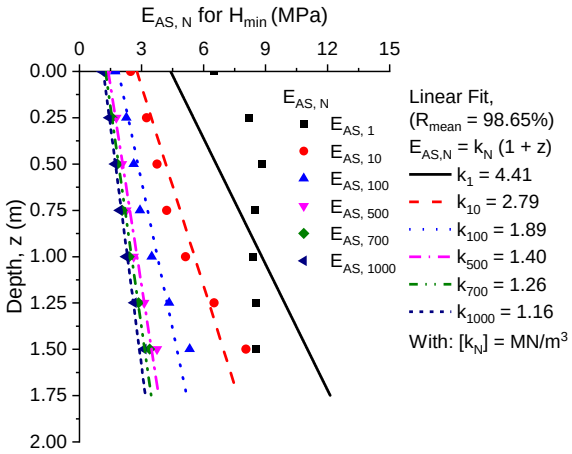

(a) Profiles of the absolute secant reaction modulus for H_{min}

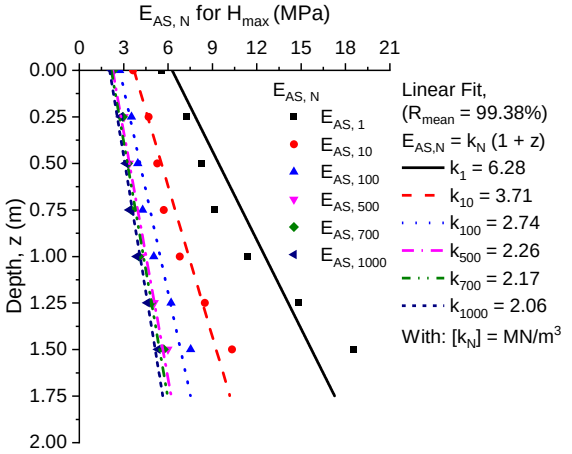

(b) Profiles of the absolute secant reaction modulus for H_{max}

Fig. 14 Profiles of the absolute secant reaction modulus

margin of 0.17 – 0.19, with a value of 0.18 corresponding to H_{mean}. After 1000 cycles, the absolute secant reaction modulus for H_{max} represents only 31% of the absolute secant modulus $E_{AS,1}$ of cycle 1 which clearly demonstrates a significant cyclic degradation of the absolute soil rigidity due to this one-way cyclic lateral loading.

The simple formulation of $E_{AS,N}$ through the power function may be used to estimate the profile of the cyclic

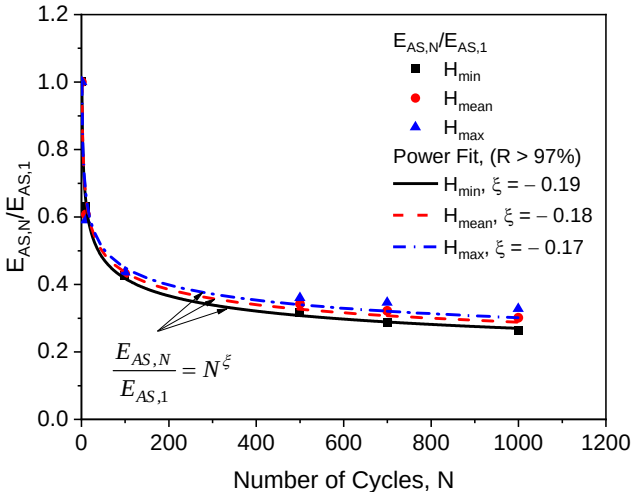

(a) Normalised absolute secant reaction modulus versus the number of cycles

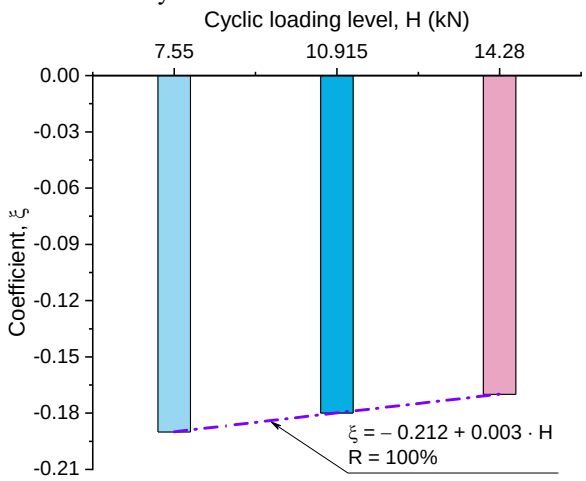

(b) Variation of the exponent ξ versus the load level

Fig. 15 Cyclic effect on the absolute secant reaction modulus

secant reaction modulus at cycle N from that of a the first cycle $E_{AS,1}$, this latter can be calculated by linear correlation with the limit pressure p_l (see Fig. 16(a) and Eq. (22)). As shown in Fig. 16(b), the multiplier λ is also linearly dependent on the loading level (see Eq. (23)).

$$E_{AS,1} = \lambda \cdot P_l \tag{22}$$

$$\lambda = 32.93 + 3.96 \cdot H \tag{23}$$

5. Numerical modelling of the cyclic loading

5.1 Finite element model of beam on elastic soil

As depicted in Fig. 17, two-dimensional finite element model in ABAQUS software was adopted. The pile is represented by a beam by means of the 2-node beam elements of type: "B21: A 2-node linear beam in a plane". By applying the principle of beam on elastic foundation (Winkler 1867), the soil around the pile is represented by

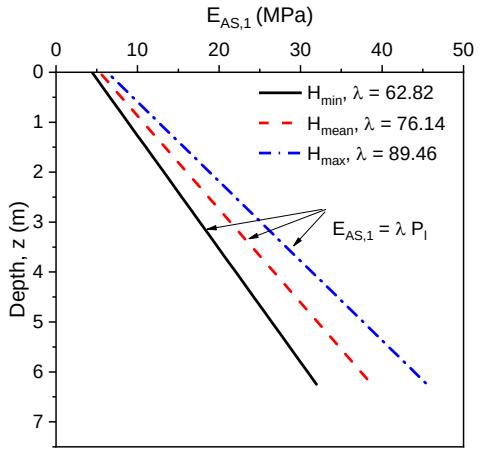

(a) Profiles of first cycle absolute secant reaction modulus

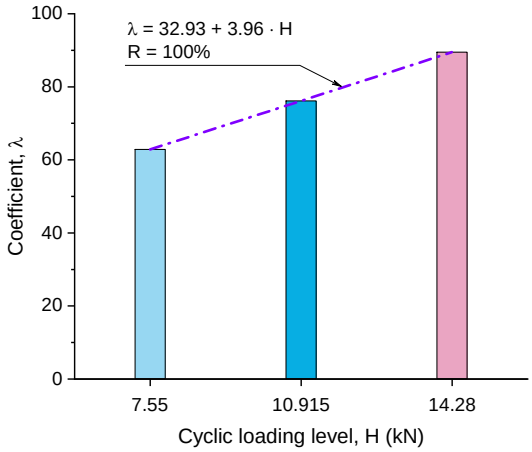

(b) Variation of the multiplier λ versus the load level

Fig. 16 Experimental bending moment profiles

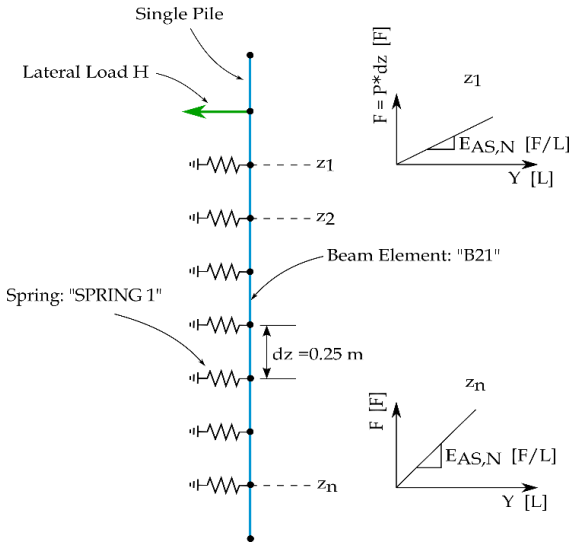

Fig. 17 Scheme of the 2D-FEM model of beam on elastic foundation

independent linear springs, the spring stiffness constant at a depth z is equal to the absolute cyclic secant modulus $E_{AS,N}$ at cycle N, multiplied by the segment length dz, which represents the height of the soil layer corresponding to

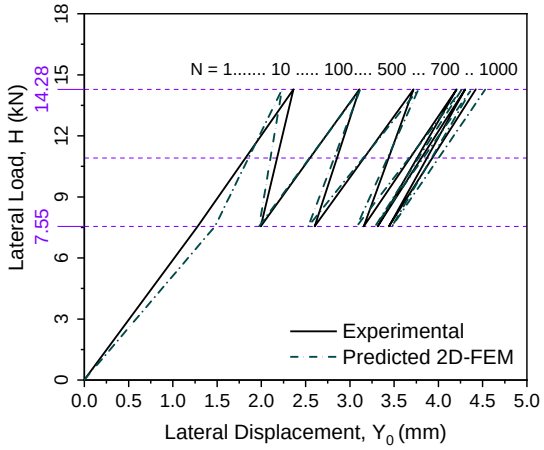

(a) Cyclic pile displacements at the mudline predicted by 2D-FEM model

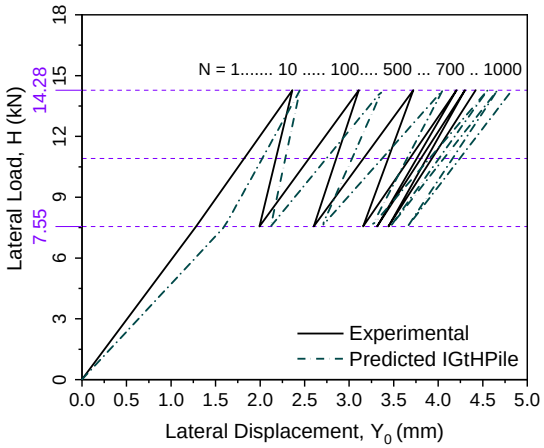

(b) Cyclic pile displacements at the mudline predicted by IGtHPile software model

Fig. 18 Cyclic pile displacements at the mudline, experimental versus numerical results

$E_{AS,N}$. In the present case, dz =0.25 m, and the pile nodes are connected directly to the surrounding soil by springs of type: "SPRING 1: connect points to ground" from ABAQUS software elements library.

Cycle-by-cycle computation was carried out to predict the pile response at each cycle N, and in order to account for the accumulated permanent deformations caused by cyclic loading, the spring stiffness constant has been changed for each cycle in accordance with the power law of degradation (see Eq. (21)). As shown in Fig. 18(a), cyclic pile displacements at the mudline for all the cycles are very well predicted.

Moreover, in Figs. 19 and 20 corresponding respectively to deflection and the bending moment profiles for H_{max} after 1 cycle and 1000 cycles, we may notice that the 2D-FEM-based profiles are in accordance with the experimental profiles, which leads to conclude that this cycle-by-cycle computation, based on a simple 2D-FEM model, predicts well the cyclic response of the test pile.

5.2 Load transfer curves-based model

Another possibility of using a simple numerical model

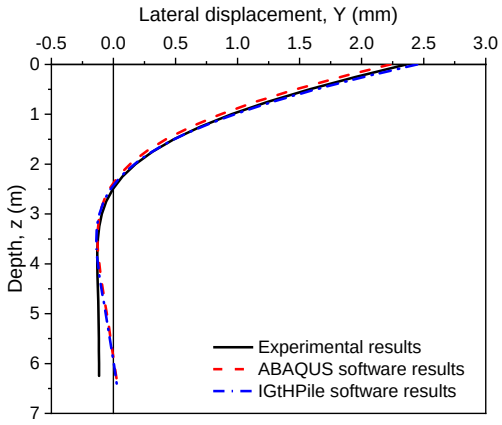

(a) Pile displacements for H_{max} after 1 cycle

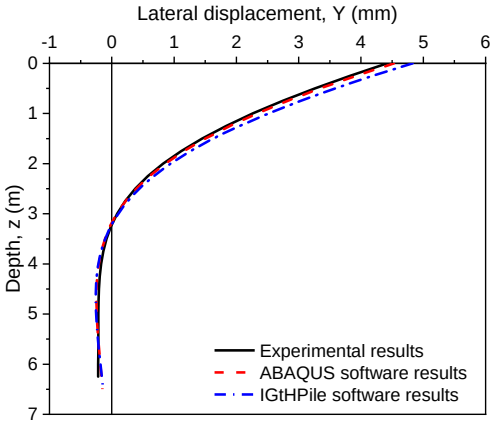

(b) Pile displacements for H_{max} after 1000 cycles

Fig. 19 Pile lateral displacements, experimental versus numerical results

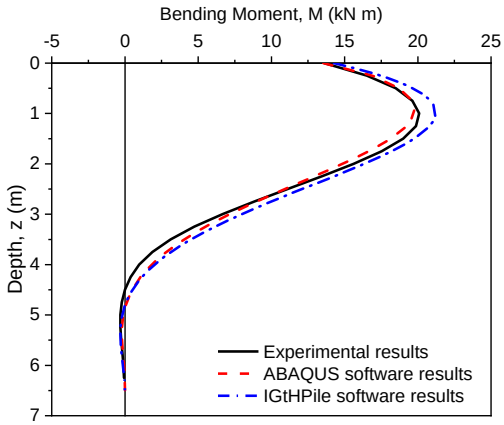

(a) Pile bending moment for H_{max} after 1 cycle

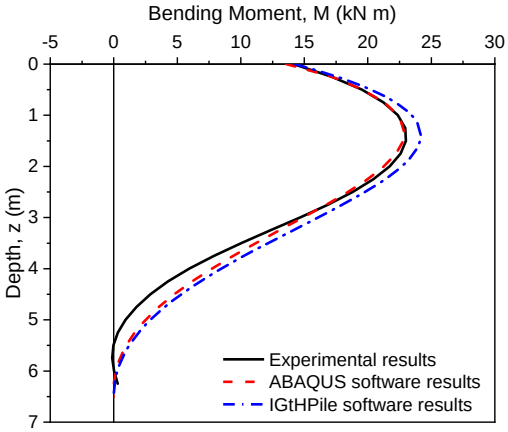

(b) Pile bending moment for H_{max} after 1000 cycles

Fig. 20 Pile bending moment, experimental versus numerical results

to predict the cyclic pile response is using a load-transfer curves method and introducing the cyclic absolute secant reaction modulus $E_{AS,N}$ as parameter characterizing the soil absolute lateral stiffness. IGtHPile software developed by The Institute of Geotechnical Engineering (IGtH), Leibniz Universität Hannover, Germany, dedicated to the design of axially and laterally loaded piles and based on the load transfer curves theory (method of *t-z*, *q-z*, P-Y curves) was used in this regard.

The beam on elastic foundation method is applied where the pile is represented by a deformable beam. For the surrounding soil, the absolute secant modulus $E_{AS,N}$ was used to simulate the lateral reaction for N loading cycles, such as the profile of $E_{AS,N}$ is introduced as linear profile (see Eq. (24)), where The gradient k_N may be easily determined from the Fig. 14 or by Eqs. (21)-(23).

$$E_{AS,N} = k_N \cdot z \tag{24}$$

Cycle-by-cycle computation was carried out and as illustrated by Fig. 18(b), for cyclic pile displacements at the mudline, a reasonable agreement was found with some discrepancy increasing with the number of cycles. Figs. 19 and 20 show also good prediction of the cyclic pile response in terms of displacement profiles as well as bending moment along the pile, through this simple model of load-transfer curves theory.

The good predictive capability of these two numerical models, based on the concept of the cyclic secant reaction modulus $E_{AS,N}$, demonstrate the possibility to simulate the cyclic response by simple numerical models. It is worth mentioning this cycle-by-cycle computation is not adapted for a practical analysis of the cyclic response for large number of cycles.

6. Conclusions

The analysis of the behaviour of a single pile under one-way cyclic lateral loading in a bi-layered soil leads to the following conclusions:

The maximum bending moment M_{max} increases logarithmically with the number of cycles N, and this increase is inversely proportional to the loading level.

The pile deflection Y_0 at the mudline shows a cumulative increase in logarithmic form with the number of cycles N, this increase depends linearly on the cyclic loading level. The pile absolute stiffness K_{AH} degrades as a power function with the number of cycles N, while the relative stiffness K_{RH} shows a minimal linear increase with the number of cycles N.

The cyclic P-Y curves are constructed, and the cyclic degradation of soil stiffness is analysed in terms of the

absolute secant modulus of $_{EAS,N}$ of lateral subgrade reaction. This latter degrades in power form with number of cycles *N*.

Based on the concept of the cyclic secant reaction modulus $E_{AS,N}$, two simple numerical models, namely a 2D-FEM model and a load-transfer curves method, were used to predict the cyclic response of the test pile. Cycle-by-cycle calculations based on these models produced accurate predictions of pile displacements and bending moment along the pile shaft for all cycles.

Acknowledgments

The authors are thankful to the scientific directorate of the IFSTTAR to provide them an official permission to use the experimental data of the site Plancoët.

References

Abadie, C. and Byrne, B, (2014). "Cyclic loading response of monopile foundations in cohesionless soils", *Physical Modelling in Geotechnics - Proceedings of the 8th International Conference on Physical Modelling in Geotechnics (ICPMG2014)*, Perth, Australia. https://doi.org/10.1201/b16200.

Adeel, M.B., Aaqib, M., Pervaiz, U., Rehman, J.U. and Park, D. (2022), "Numerical response of pile foundations in granular soils subjected to lateral load", *Geomech. Eng*., **28**(1), 11-23. https://doi.org/10.12989/gae.2021.28.1.011.

AFNOR (2005)m Reconnaissance et essais géotechniques - Dénomination, description et classification des sols - Partie 2 : principes pour une classification.

AFNOR (2012), Justification des ouvrages géotechniques - Normes d'application nationale de l'Eurocode 7 - Fondations profondes. Norme française NF P94-262.

Allotey, N. and El Naggar, M. H. (2008), "A numerical study into lateral cyclic nonlinear soil–pile response", *Can. Geotech. J*., **45**(9), 1268-1281. https://doi.org/10.1139/T08-050.

API (2007), RP 2A-WSD Recommended practice for planning, designing, and constructing fixed offshore platforms: working stress design. American Petroleum Institute.

Ashour, M. and Norris, G. (2000), "Modeling lateral soil-pile response based on soil-pile interaction", *J. Geotech. Geoenviron. Eng*., **126**(5), 420-428. https://doi.org/10.1061/(ASCE)1090-0241(2000)126:5(420).

Baguelin, F. and Jezequel, J. (1972), "Etude experimentale du comportement de pieux sollicites horizontalement", *Bull. Liais. Lab. Ponts Chauss*., (62), 308-322.

Baguelin, F., Frank, R. and Jezequel, J.F. (1989), "Interprétations d'essais de chargement latéral d'un pieu isolé", *Proceedings of the 12th International Conference on Soil Mechanics and Foundation Engineering*, Rio De Janeiro, Brazil. https://www.issmge.org/publications/publication/interpretations-dessais-de-chargement-lateral-dun-pieu-isole.

Baguelin, F., Meimon, Y. and Jezequel, J.F. (1985), "Chargements latéraux sur un groupe des pieux", *Proceedings of the 11th International Conference on Soil Mechanics and Foundation Engineering*, San Francisco, USA.

Barari, A., Zeng, X., Rezania, M. and Ibsen, L.B. (2021), "Three-dimensional modeling of monopiles in sand subjected to lateral loading under static and cyclic conditions", *Geomech. Eng*., **26**(2), 175-190. https://doi.org/10.12989/gae.2021.26.2.175.

Bouafia, A. (1994), "Étude expérimentale du chargement latéral cyclique répété des pieux isolés dans le sable en centrifugeuse", *Can. Geotech. J*., **31**(5), 740-748. https://doi.org/10.1139/t94-085.

Briaud, J.L. (2013), Geotechnical Engineering: Unsaturated and Saturated Soils, John Wiley & Sons, Hoboken, New Jersey. https://doi.org/10.1002/9781118686195.

Cassan, M. (1978), Les essais in situ en mécanique des sols. 1. Realisation et interpretation. Eyrolles, Paris.

CCTG (1993), Règles techniques de conception et de calcul des fondations des ouvrages de génie civil, Fascicule 62 titre V. Ministère de l'Equipement, du Logement et des Transports.

Chiou, J.S., Xu, Z.W., Tsai, C.C. and Hwang, J.H. (2018), "Lateral cyclic response of an aluminum model pile in sand", *Mar. Georesour. Geotech*., **36**(5), 554-563. https://doi.org/10.1080/1064119X.2017.1351504.

Chong, S.H., Shin, H.S. and Cho, G.C. (2019), "Numerical analysis of offshore monopile during repetitive lateral loading", *Geomech. Eng*., **19**(1), 79-91. https://doi.org/10.12989/gae.2019.19.1.079.

Cuéllar, P. (2011), "Pile foundations for offshore wind turbines: Numerical and experimental investigations on the behaviour under short-term and long-term cyclic loading", Doctoral Thesis in German, Technische Universität Berlin, Fakultät VI - Planen Bauen Umwelt, Berlin, Germany. https://doi.org/10.14279/depositonce-2760.

Dassault Systèmes Simulia "ABAQUS 2016 Documentation", [computer program] Available at: http://130.149.89.49:2080/v2016/index.html

Degny, E., Frank, R. and Hadjadji, T. (1994), "Interprétation d'essais de pieux sous charges latérales", *Proceedings of the 13th ICSMFE*, New-Delhi, India.

Duncan, J.M. and Chang, C.Y. (1970), "Nonlinear analysis of stress and strain in soils", *J. Soil Mech. Found. Div*., **96**(5), 1629-1653. https://doi.org/10.1061/JSFEAQ.0001458.

Fenu, L., Briseghella, B. and Marano, G.C. (2019), "Simplified method to design laterally loaded piles with optimum shape and length", *Struct. Eng. Mech*., **71**(2), 119-129. https://doi.org/10.12989/sem.2019.71.2.119.

Gazioglu, S.M. and O'Neill, M.W. (1984), "Evaluation of P-Y relationships in cohesive soils", Analysis and Design of Pile Foundations, ASCE, 192-213.

Hadjadji, T., Frank, R. and Degny, E. (2002), Analyse du comportement expérimental de pieux sous chargements horizontaux. Géotechnique et risques naturels, Laboratoire Central des Ponts et Chaussées (LCPC), France.

Hettler, A. (1981), "Verschiebungen starrer und elastischer Gründungskörper in Sand bei monotoner und zyklischer Belastung", Doctoral Thesis [in German], Veröffentlichungen des Instituts für Bodenmechanik und Felsmechanik der Universität Karlsruhe, Germany, Heft 90, 127.

Hinz, P. (2009), "Beurteilung des Langzeitverhaltens zyklisch horizontal belasteter Monopile-Gründung." Doctoral Thesis [in German], Mitteilungen aus dem Fachgebiet Grundbau und Bodenmechanik, Universität Duisburg-Essen, Germany, Heft 37, 182.

IGtHPile Version 3.01 (2015), "Design software for axially and laterally loaded foundation piles", Institute and for Geotechnical Engineering (IGtH), Leibniz University Hannover, Germany. [computer program]. Available at: https://www.igth.uni-hannover.de/en/research/igth-pile/

Klinkvort, R.T. and Hededal, O. (2013), "Lateral response of monopile supporting an offshore wind turbine", *Proceedings of the Institution of Civil Engineers - Geotechnical Engineering*, **166**(2), 147-158. https://doi.org/10.1680/geng.12.00033.

LeBlanc, C., Houlsby, G.T. and Byrne, B.W. (2010), "Response of stiff piles in sand to long-term cyclic lateral loading", *Géotechnique*, **60**(2), 79-90. https://doi.org/10.1680/geot.7.00196.

Li, Z., Haigh, S.K. and Bolton, M.D. (2010), "Centrifuge modelling of mono-pile under cyclic lateral loads", *Proceedings of the 7th International Conference on Physical Modelling in Geotechnics*, Zurich.

Lin, S.S. and Liao, J.C. (1999), "Permanent strains of piles in sand due to cyclic lateral loads", *J. Geotech. Geoenviron. Eng.*, **125**(9), 798-802. https://doi.org/10.1061/(ASCE)1090-0241(1999)125:9(798).

Long, J.H. and Vanneste, G. (1994), "Effects of cyclic lateral loads on piles in sand", *J. Geotech. Eng.*, **120**(1), 225-244. https://doi.org/10.1061/(ASCE)0733-9410(1994)120:1(225).

Matlock, H. (1970), "Correlation for design of laterally loaded piles in soft clay", *Proceedings of the 2nd Offshore Technology Conference*, Houston, Texas, April. https://doi.org/10.4043/1204-MS.

Meimon, Y., Baguelin, F. and Jezequel, J. (1986), "Comportement d'un groupe de pieux sous chargement latéral monotone et cyclique de longue durée", 3e Colloque international sur les méthodes numériques de calcul des pieux pour les ouvrages en mer, Nantes, France.

Ménard, L. (1967), Règles d'utilisation des techniques pressiométriques et d'exploitation des résultats obtenus pour le calcul des fondations. Notice générale D60.

Nicolai, G. and Ibsen, L.B. (2015), "Investigation on monopiles behavior under cyclic lateral loads in dense sand", *Proceedings of the 25th International Ocean and Polar Engineering Conference*, Kona, Big Island, Hawaii, USA.

Niemunis, A., Wichtmann, T. and Triantafyllidis, Th. (2005), "A high-cycle accumulation model for sand", *Comput. Geotech.*, **32**(4), 245-263. https://doi.org/10.1016/j.compgeo.2005.03.002.

Norris, G. (1986), "Theoretically based BEF laterally loaded pile analysis", Proceedings of the 3rd international conference on numerical methods in offshore piling, Paris, France.

Peralta, P. (2010), "Investigations on the behavior of large diameter piles under long-term lateral cyclic loading in cohesionless soil", Institut für Geotechnik (IGtH), Leibnitz Universität Hannover, Hannover.

Poulos, H.G. (1988), Marine geotechnics. Unwin Hyman, London.

Reese, L.C. and Impe, W.F.V. (2010), Single piles and pile groups under lateral loading, CRC Press, Leiden ; Boca Raton. https://doi.org/10.1201/b17499

Reese, L.C. and Welch, R.C. (1975), "Lateral loading of deep foundations in stiff clay", *J. Geotech. Eng. Div. - ASCE*, **101**(7), 633-649.

Reese, L.C., Cox, W.R. and Koop, F.D. (1974), "Analysis of laterally loaded piles in sand", *Proceedings of the 6th Annual Offshore Technology Conference*, Houston, Texas, May. https://doi.org/10.4043/2080-MS.

Reese, L.C., Cox, W.R. and Koop, F.D. (1975), "Field testing and analysis of laterally loaded piles in stiff clay", *Proceedings of the 7th Annual Offshore Technology Conference*, Houston, Texas, May. https://doi.org/10.4043/2312-MS.

Rosquoët, F., Thorel, L., Garnier, J. and Canepa, Y. (2007), "Lateral cyclic loading of sand-installed piles", *Soils Found.*, **47**(5), 821-832. https://doi.org/10.3208/sandf.47.821.

Smith, T.D. (1983), "Pressuremeter design method for single piles subjected to static lateral load", PhD thesis, Texas A & M University. https://hdl.handle.net/1969.1/DISSERTATIONS-541480.

Staubach, P., Machaček, J., Sharif, R. and Wichtmann, T. (2021), "Back-analysis of model tests on piles in sand subjected to long-term lateral cyclic loading: Impact of the pile installation and application of the HCA model", *Comput. Geotech.*, **134**, 104018. https://doi.org/10.1016/j.compgeo.2021.104018.

Staubach, P., Machaček, J., Tafili, M. and Wichtmann, T. (2022), "A high-cycle accumulation model for clay and its application to monopile foundations", *Acta Geotech.*, **17**, 677-698. https://doi.org/10.1007/s11440-021-01446-9.

Staubach, P., Machaček, J., Tschirschky, L. and Wichtmann, T. (2022), "Enhancement of a high-cycle accumulation model by an adaptive strain amplitude and its application to monopile foundations", *Int. J. Numer. Anal Methods*, **46**, 315-338. https://doi.org/10.1002/nag.3301.

Sullivan, W.R., Reese, L.C. and Fenske, C.W. (1980), "17. Unified method for analysis of laterally loaded piles in clay", *Numer. Method. Offshore Pili.*, 135-146. https://www.icevirtuallibrary.com/doi/abs/10.1680/nmiop.00865.0017.

Swane, I.C. (1983), The Cyclic Behaviour of Laterally Loaded Piles. University of Sydney.

Tasan, H.E. (2011), "Zur Dimensionierung der Monopile-Gründungen von Offshore-Windenergieanlagen", Doctoral Thesis [in German], Technische Universität Berlin, Fakultät VI - Planen Bauen Umwelt, Berlin, Germany, 174. https://doi.org/10.14279/depositonce-2786.

Tuladhar, R., Maki, T., and Mutsuyoshi, H. (2008). "Cyclic behavior of laterally loaded concrete piles embedded into cohesive soil", *Earthq. Eng. Struct. D.*, **37**(1), 43-59. https://doi.org/10.1002/eqe.744.

Winkler, E. (1867), "Die Lehre von der Elasticitaet und Festigkeit: mit besonderer Rücksicht auf ihre Anwendung in der Technik für polytechnische Schulen, Bauakademien, Ingenieure, Maschinenbauer, Architekten, etc", [In German], Domenicus, Prag, 424.

Yang, Y., Gao, X., Wu, W. and Xing, K.A. (2021), "A simplified method for analysis of laterally loaded piles considering cyclic soil degradation", *Adv. Civil Eng.*, 9096540. https://doi.org/10.1155/2021/9096540.

JS